Polymer Bulletin
https://doi.org/10.1007/s00289-019-02847-3

ORIGINAL PAPER

Aluminum triflate-cocatalyzed radical copolymerization of styrene and ethyl acrylate

Upenyu Guyo[1] · **Daniel P. Otto**[1] · **Desmond A. Young**[1] · **Hermanus C. M. Vosloo**[1]

Received: 9 January 2019 / Revised: 2 April 2019 / Accepted: 17 June 2019

Abstract

Various random copolymers, poly(styrene-*co*-ethyl acrylate), were synthesized by free radical bulk copolymerization cocatalyzed by aluminum triflate ($Al(OTf)_3$). The experimental conditions for the polymerization reactions, which include the amount of cocatalyst, polymerization time and ratio of styrene to ethyl acrylate, were investigated. The copolymer molecular weights were determined by gel permeation chromatography coupled to multi-angle laser light scattering. Compositional analysis was performed using proton nuclear magnetic resonance spectrometry. Electron paramagnetic resonance spectroscopy was also used to study the radical species which form in the presence or absence of $Al(OTf)_3$. Kinetic studies were performed by determining monomer conversions as a function of time on gas chromatography. It was found that $Al(OTf)_3$ accelerated the rate of polymerization significantly while also increasing the polymer molecular weights for a given conversion compared to the reactions where the triflate was absent. $Al(OTf)_3$ can be a significantly more cost-effective and abundant alternative polymerization cocatalyst compared to some of the rare lanthanide triflates.

Keywords Copolymerization · Ethyl acrylate · Styrene · Aluminum triflate · Radical stability · GPC · NMR · EPR

Electronic supplementary material The online version of this article (https://doi.org/10.1007/s00289-019-02847-3) contains supplementary material, which is available to authorized users.

✉ Upenyu Guyo
upguyo@gmail.com

[1] Research Focus Area for Chemical Resource Beneficiation, Catalysis and Synthesis Research Group, North-West University, Potchefstroom 2520, South Africa

Published online: 22 June 2019

Introduction

The copolymerization of polar vinyl monomers, for example the acrylates with apolar 1-alkenes, can incorporate both monomer properties in a polymer with novel properties [1]. Considerable research has been done on copolymerization of styrene (S) and ethyl acrylate (EA) in bulk, emulsion and solution, but very little has been done in the presence of cocatalyst [2, 3]. Scheme 1 illustrates the copolymerization of S and EA as an example of a copolymerization reaction where an apolar and a polar monomer are copolymerized.

Cocatalysts provide a means to abridge these challenges, and especially Lewis acids have been used successfully in numerous homo- and heterogeneous catalyzed reactions [4]. A Lewis acid cocatalyst typically comprises a metal center, which could be coordinated by ligands, that acts as an electron pair acceptor from nucleophilic species [4]. Classic Lewis acids such as $AlCl_3$ unfortunately suffer from poor water tolerance and easily decompose in the presence of water [5]. Employment of water-tolerant Lewis acid cocatalysts, for instance metal triflates [6], can overcome the instability in water. Recently, aluminum triflate ($Al(OTf)_3$) successfully demonstrated an improvement in the yield of the polycondensation reactions of novel phenylenediamine-derived monomers [7–9].

Other polymers that have also been synthesized using metal triflates include the employment of scandium triflate for the copolymerization of (meth-)acrylates and 1-alkenes [1], a series of rare earth metal triflate in the polymerization of *N*-isopropylacrylamide, acrylamide and *N,N*-dimethylacrylamide [10], the utilization of scandium triflate in the copolymerization of methyl acrylate and methyl methacrylate with 1-alkenes [11], polymerization of *n*-butyl acrylate in the presence of scandium triflate [12] and the polymerization of methyl methacrylate, ethyl methacrylate, isopropyl methacrylate and 2-methoxyethyl methacrylates using various rare earth lanthanide triflates [13].

The mechanism by which Lewis acids catalyze polymerization reactions is a subject of contention. Concerning the polar vinyl monomers, for example acrylates, the general consensus is that the vacant metal orbital of the Lewis acid can coordinate to the carbonyl oxygen of the (meth-)acrylate [1, 12, 14]. This coordination will deshield the vinyl bond of the monomer by withdrawing the unpaired oxygen electrons to the vacant orbital which shows up in the NMR spectra as downfield shifts where nuclei are in close vicinity to the coordinating site [12]. Subsequently, the

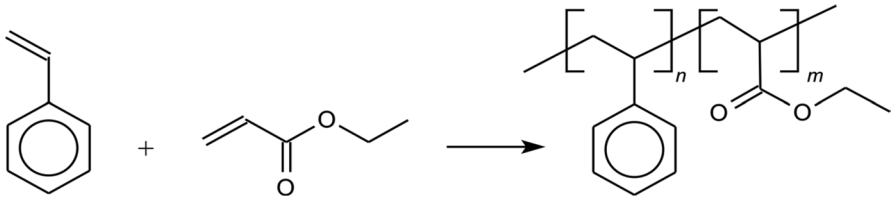

Scheme 1 Copolymerization of S with EA to yield the poly(S-*co*-EA). The $Al(OTf)_3$ was present or absent depending on the chosen reaction conditions

vinyl bond is also more susceptible to nucleophilic attack by electron-donating monomers in its proximity such as reported for 1-alkenes. The Lewis acid coordination to the acrylic monomer facilitates the electron withdrawing from the otherwise less reactive 1-alkene species that subsequently become energetically favorable for copolymerization with the acrylic monomer [15]. Subsequently, more efficient polymerization of alkenes will potentially be observed using the appropriate Lewis acid as demonstrated, for example for isobutylene [16], propylene [17] and ethylene [18].

If the initiator already generated a monomer radical, this coordination effect to the Lewis acid metal center will therefore render the monomer in a so-called activated state and will promote its reactivity. It should be considered that coordinated monomer and monomer radical species are both more reactive than the uncoordinated monomer [19]. The mechanism by which the Lewis acid coordinates to carbonyl groups in this study is via π- and σ-type interactions [20].

The effect of Lewis acids on more apolar vinyl monomers including S and 1-alkenes is poorly understood. A number of studies suggested that the vacant metal orbital also coordinates, however, directly to the vinyl bond and not to a polar site on the monomer such as the carbonyl oxygen of (meth-)acrylates. This observation is apparently seen best in apolar solvents such as toluene since polar, protic solvents suppress Lewis acidity that prevents coordination or degrades the Lewis acid. To prevent degradation, pH-buffered aqueous solutions have proven its worth in the prevention of degradation of some classic Lewis acids including $AlCl_3$, $TiCl_4$ and $SnCl_4$ [21]. In lieu of the desire to develop more environmentally benign industrial processes, more water-tolerant Lewis acids may be of great value and also facilitate chemical reactions in water which would otherwise only be possible in aprotic media. Furthermore, it could render certain industrial processes more robust in terms of water tolerance [22].

This study investigates one of the first employments of $Al(OTf)_3$ as a cocatalyst in the copolymerization of S and EA. $Al(OTf)_3$ is a water-tolerant Lewis acid with a high degree of Lewis acidity as conferred by the aluminum center. Therefore, it does not suffer from decomposition in water or the impairment of coordination between the metal center and for instance carbonyl oxygen atoms that is often caused by water. The positive effect of the triflate on the kinetics of the copolymerization study is reported, and its advantageous interplay regarding molecular weight is demonstrated. In addition, an attempt was made to gain mechanistic insight into the effect of the triflate on the copolymerization reaction as gleaned from NMR and EPR studies.

Experimental

Materials

EA (99%, SASOL) and S (Sigma-Aldrich) were purified by running through a column packed with activated basic aluminum oxide (Sigma-Aldrich) to remove the inhibitor. Benzoyl peroxide (BPO) (Sigma) and $Al(OTf)_3$ (97%, Sigma) were used as received. Toluene (Absolute, Sigma) was used as received; methanol (Rochelle

Chemicals) and ethanol (MINEMA) were purified using methods available in the literature. 2-Methyl-2-nitrosopropane (MNP) (ESR grade, Aldrich) was used as radical trap.

Synthesis procedure

Polymerization reactions were carried out in a 30-mL stainless steel autoclave reactor equipped with safety valves, a stirrer and a heating mantle. The reactor which was first dried and purged with nitrogen was charged with requisite quantities of reagents. For homopolymerization reactions, S or EA (0.05 mol) was charged into the reactor together with 10 mL of toluene.

For copolymerization reactions, the reactor was charged with 1:1 volume ratio of S and EA together with 10 mL of toluene. The contents were purged with nitrogen before being brought to polymerization temperature (70 °C) while stirring (400 rpm). BPO (2% w/w) was used as the initiator in all the reactions. The reaction mixture was stirred under nitrogen for 3 h. The effects of $Al(OTf)_3$, temperature, monomer concentrations on yield, percentage monomer incorporation and molecular weight distribution of the copolymers were established. At the end of the reaction, the polymers were precipitated in excess acidified methanol, filtered, and washed with methanol. The homopolymers were insoluble in acetone, and hence the copolymers were extracted in acetone followed by re-precipitation in excess methanol. The homopolymer-free product was dried under vacuum at 40 °C overnight.

Kinetic studies

Kinetic studies were conducted by carrying out the copolymerization reactions as described in the "Sample characterization and analysis" section using toluene as solvent. The primary focus was to show the effect of $Al(OTf)_3$ on the rate of copolymerization reaction as measured by the rate of consumption of the feed monomers. Two reaction setups, one with and the other without $Al(OTf)_3$, were employed at 70 °C. A reference sample was drawn at t_0. Conversion was monitored by GC through regular sampling up to full conversion before quenching with methanol. A portion of the sample for GC analysis was passed through a small column packed with basic alumina. The remainder of the sample was filtered through alumina, precipitated and dried followed by GPC analysis.

Sample characterization and analysis

Attenuated total reflectance Fourier-transform infrared spectroscopy (ATR-FTIR)

Fourier-transform infrared spectra were recorded at room temperature on a Bruker Alpha ATR-FTIR spectrometer in the region 4000–400 cm^{-1}. The spectrometer was equipped with a micro-ATR sampling accessory with a ZnSe crystal and made use of a He–Ne laser operating at 632.8 nm. Thirty-two scans with a spectral resolution of 4 cm^{-1} were collected for each sample.

Proton nuclear magnetic resonance spectroscopy (^{1}H NMR)

NMR spectra (^{1}H and ^{13}C) were obtained with a 600 SB Ultra Shield Bruker Ultrashield™ Plus NMR spectrometer operating at 600 MHz. Unless mentioned otherwise, deuterated chloroform was used as solvent. Tetramethylsilane (TMS) was the internal standard.

Copolymer compositions were determined by ^{1}H NMR comparison of the integrated intensities of phenyl protons of S resonance signals (6.5–7.3 ppm) and those of the methylene protons nearest to the oxygen atom of the ester group of EA (3.4–4.1 ppm). These signals appeared to be unaffected by the solvent signals. Percentage EA incorporation is given by Eq. (1):

$$\%\mathrm{EA} = \frac{A(\mathrm{EA})(3.4 - 4.2\,\mathrm{ppm})/2}{A(\mathrm{EA})(3.4 - 4.2\,\mathrm{ppm})/2 + A(\mathrm{S})(6.5 - 7.3\,\mathrm{ppm})/5}, \tag{1}$$

where A(EA) is the area of the resonance signal characteristic of the two protons on the methylene close to ester group of EA and A(S) is the area of the resonance signal of the five protons on the S phenyl ring. The characteristic regions of the chemical shifts (ppm) of the proton signals are given as coefficients in the equation.

Thermal characterization of samples

Thermal analysis of the polymers was conducted using TGA and DSC techniques. DSC measurements were carried out for the polymers at temperatures from −50 to 200 °C using modulated differential scanning calorimetry with a DSC 25 (Advanced Laboratory Solutions, Germany) at a heating rate of 10 °C/min under a nitrogen atmosphere). TGA was recorded on a thermal analyzer TGA550 (Advanced Laboratory Solutions, Germany) at a heating rate of 10 °C/min in the presence of air.

Electron paramagnetic resonance (EPR) spectroscopy

A Bruker EMX Plus spectrometer was employed in all EPR studies. The measurement conditions were set as follows: center field at 3500 G, sweep field at 2000 G, static field at 2500 G, frequency at 9.785 GHz, power of 20 mW, modulation frequency at 100 kHz, modulation amplitude of 10 G, conversion time of 4 ms, a sweep time of 20 s and a resolution of 5000×.

All the EPR experiments were performed using these measurement conditions. Experiment 1 (Exp. 1) employed only S (0.008 mol) as monomer, BPO as initiator (9.4% w/w) and MNPD (~20% w/w) as radical trap. Exp. 2 employed the same conditions as in Exp. 1, however, with the addition of $Al(OTf)_3$ (0.02 mol%). Exps. 3 and 4 repeated these procedures substituting EA (0.008 mol) for S. Exps. 5 and 6 repeated the procedures for the comonomer combinations.

Gas chromatography (GC)

Gas chromatographic analyses were performed on an Agilent Gas Chromatograph (6850 Series), equipped with a flame ionization detector. An HP-5 column (length 30 m × 0.25 mm ID × 0.25 mm thickness) was used in the analysis with N_2 at a flow rate of 1.5 mL/min as the carrier gas.

Gel permeation chromatography (GPC)

Molecular weight of the copolymers was determined using gel permeation chromatography (HP 1100 series chromatograph, Waldbronn, Germany) with double detection. Multi-angle laser light scattering (MALLS) detection was performed with DAWN® DSP photometer (Wyatt Technologies Corp., Santa Barbara, CA) at 632.8 nm and refractive index (RI) concentration detection with an Agilent RI detector. Data analysis and detector signal overlay were performed using ASTRA™ 4.73 software with the Zimm formalism (Wyatt Technologies Corp., Santa Barbara, CA). Polymer samples were prepared at a concentration of approximately 5 mg/mL in HPLC-grade tetrahydrofuran (THF) (Sigma-Aldrich, Johannesburg, South Africa). The samples were filtered through 0.45-µm PTFE syringe filters prior to injection of 100 µL of the samples.

THF was also used as elution liquid at a flow rate of 1 mL/min. A 0.45-µm inline filter preceded the coupling to the GPC columns. The column temperature of RI optical unit cell was maintained at 35 °C. Three 7.8 × 300 mm GPC columns were coupled in series: an Agilent PL gel, 10 µm with a molecular weight inclusion range of 40,000–4,000,000 g/mol (Chemetrix, Midrand, South Africa), an Agilent PL gel mixed-bed type C 5 µm (Chemetrix) with a molecular weight inclusion range of 300–2,000,000 g/mol and a Phenomenex Phenogel (Separations, Randburg, South Africa) 5 µm column with an inclusion range of < 5000 g/mol.

Equation (2) is used to compute absolute molecular weight of the sample via the software [23]:

$$\frac{R_\theta}{Kc} = MP(\theta) - 2A_2cM^2P^2(\theta) + \cdots, \tag{2}$$

where M is the absolute molecular weight measured for a discrete slice in chromatogram, R_θ is the excess Rayleigh scattering of the sample at the angle, θ. The wavelength-dependent particle scattering factor is given by $P(\theta)$. The concentration of the particles in the sample (RI detection) for a discrete slice is given by c. A_2 is the second virial coefficient indicating the volume exclusion effect due to high sample concentration effecting clustering—this value is negligible at the sample concentration used here. K is the detector signal overlay constant which is derived from Eq. (3) [23]:

$$K = \frac{4\pi^2 n_0^2}{\lambda_0^4 N_A}\left(\frac{dn}{dc}\right)^2, \tag{3}$$

where n_0 is the refractive index of the solvent (THF) at the wavelength, λ. The Avogadro number is given by N_A, and the specific refractive increment is stated by *dn/dc*.

A PS standard with a reference *dn/dc* of 0.185 was used to calculate the average *dn/dc* of the experimental sample via an online method [24] which was substituted in Eq. (2).

GPC analysis was used to determine number average molecular weight ($\overline{M}_n$), weight average molecular weight ($\overline{M}_w$), as well as the polydispersity index (PDI) of the polymers expressed as $\overline{M}_w \Big/ \overline{M}_n$.

Results and discussion

ATR-FTIR

ATR-FTIR showed absorption band at 699 cm^{-1} characteristic of the out-of-plane ring deformation of the S monomer phenyl ring and absorption band at 1729 cm^{-1} characteristic of the ester carbonyl group of EA monomer. These two spectral regions are of particular interest in the analysis of S–EA copolymers. Other observed spectral regions of interest were 2954 cm^{-1} of (C–H) and 1389 cm^{-1} of (C–O) for the ester monomer, and 3025 cm^{-1} of (C–H) for the S monomer. Figure 1 shows typical ATR-FTIR spectra for a poly(S-*co*-EA) copolymer for initial feed of 1:1 S:EA as well as pure homopolymers comprising one of the monomers.

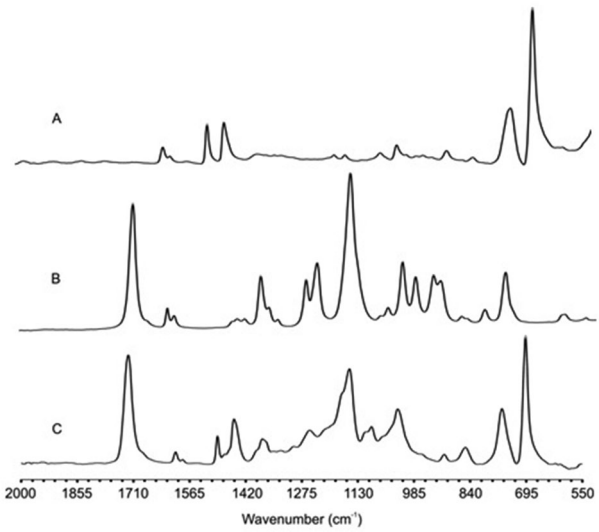

Fig. 1 Typical FTIR spectra of **a** PS, **b** PEA and **c** poly(S-*co*-EA) expanded to show the region 550–2000 cm^{-1}

^{1}H NMR

The proton NMR spectra for monomers in the absence of $Al(OTf)_3$ are presented in Fig. S3. Figure 2 depicts the ^{1}H NMR spectrum of a copolymer produced in the presence of 0.9 mol% of $Al(OTf)_3$.

The spectrum clearly shows peak broadening which is characteristic of polymeric materials. In the supporting information, spectra of the pure monomers indicate lack of line broadening. The S phenyl ring protons lie in the region of δ: 6.5–7.3 ppm, while the methylene protons of the ethoxy protons in EA in δ: 3.4–4.2 ppm. The vinyl groups of the monomers clearly reacted since the resonance signals of the vinyl protons of the monomers do not appear anymore in the downfield region. Instead, due to the saturated bonds forming between vinyl groups during polymerization, the protons become significantly more shielded and now show signals in the aliphatic region at ~ 2.1–1.0 ppm. The effect of $Al(OTf)_3$ on the monomer NMR spectra is discussed next. Figure 3 illustrates the obtained spectra.

From Fig. 3, it was observed that the triflate induced a slightly more deshielded EA spectrum compared to the neat EA spectrum. The difference spectrum indicated that virtually no overlap between the triflate-devoid and triflate-added spectrum

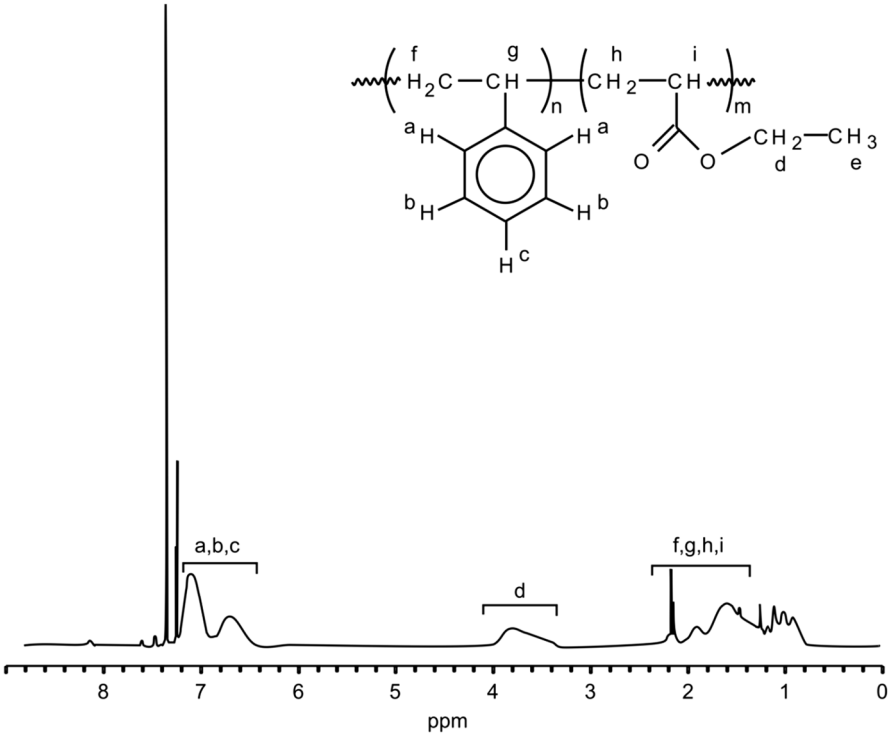

Fig. 2 Typical ^{1}H NMR spectrum of poly(S-*co*-EA) polymerized from S/EA (4:6) at 80 °C, with 10 mL toluene, $Al(OTf)_3$ (0.9 mol%), BPO (12.3% w/w) at the end of 4 h 30 min

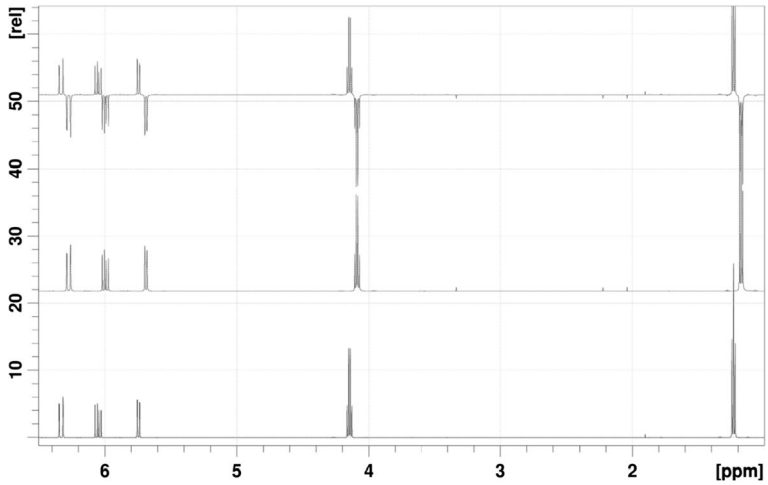

Fig. 3 Bottom ^{1}H spectrum shows EA with addition Al(OTf)$_3$ (0.9 mol%), the middle spectrum shows neat EA, and the top spectrum shows the difference spectrum obtained by subtracting the EA and EA-triflate spectra from each other

was observed. Although small the magnitude of the shifts (~0.2 ppm), other studies on Lewis acids have shown the same small-magnitude shifts and these had clear enhancements of the chain propagation kinetics. Some examples of reports where these small shifts are reported include the use of $AlCl_3$ in the polymerization of (meth-)acrylates [1] and Sc(OTf)$_3$ used in the polymerization of methyl methacrylate and methyl acrylate [10]. Figure 4 shows the effect of the triflate on the comonomer mixture.

Although small, ppm shifts are observed in the spectra depicted in Fig. 4 for the mixture in the presence of the triflate; these are confirmed from the difference spectrum that shows no overlap between the spectra obtained in the presence or absence of Al(OTf)$_3$. From this difference plot, it can also be observed that S is also affected by the triflate and that it is also slightly more shielded in the presence of the triflate. It has been reported that S conversion to PS could be accelerated by Cu(OTf)$_2$ that was either used as homogeneous catalyst or supported catalyst [25]. All these interactions indicate an interaction between the triflate and monomer which results in the slightly higher (de-)shielding of the monomer nuclei, potentially rendering the vinyl radical more available for polymerization from the acrylate side and the higher propensity of electron donation by S to increase its own reactivity. To investigate the radical species that form, ESR spectroscopy studies were performed next. The NMR studies did indicate that both monomers were affected by the presence of the triflate, and this can be investigated in more detail by radical trapping studies.

ESR spectroscopy and the effect of Al(OTf)$_3$ on radical species

Figure 5 presents the ESR spectrum of S radicals produced in the absence of aluminum triflate cocatalyst. The ESR spectrum showed a triplet which is typical of

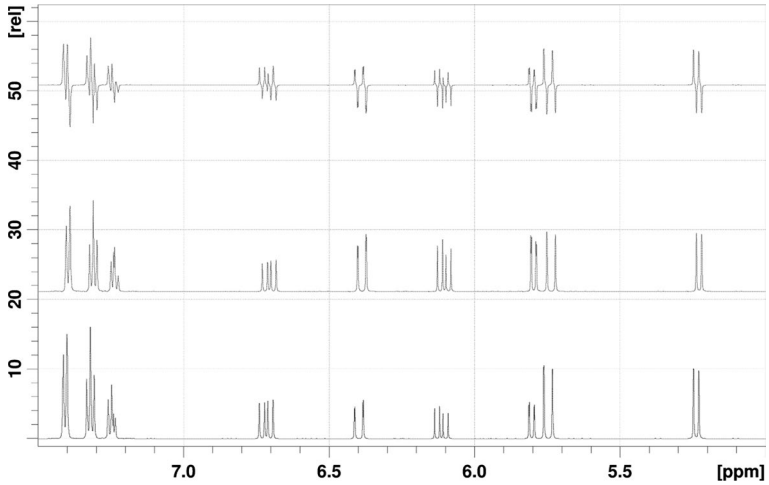

Fig. 4 Expanded ^{1}H spectrum of the monomer mixtures. The bottom spectrum shows the mixture with addition $Al(OTf)_3$ (0.9 mol%), the middle spectrum shows the monomer mixture without $Al(OTf)_3$, and the top spectrum shows the difference spectrum obtained by subtracting the mixture and mixture-triflate spectra from each other

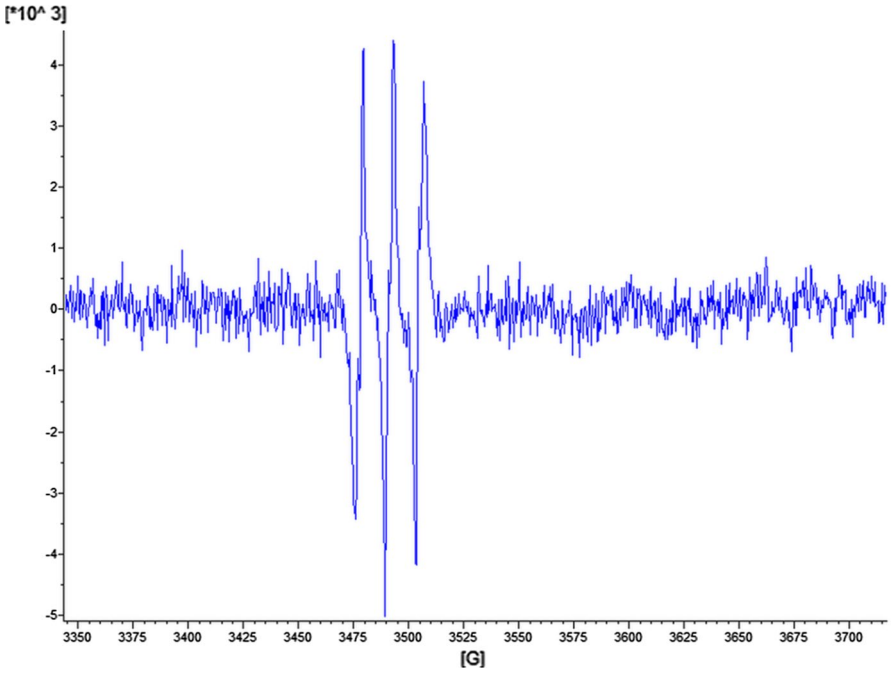

Fig. 5 EPR spectrum of S without $Al(OTf)_3$

the presence of S showing presence of a propagating radical, *, –CH_2CH*Ph–. The three-line spectrum might be due to interaction of the unpaired electron with the surrounding methylene protons [26]. According to Kajiwara [27], low intensity of the radicals implies radical instability such that the three-line spectrum might have been due to the chain radical formed by transfer reactions –CH_2C*$(Ph)CH_2$–. The radical on the chain may move to the *meta*- and *para*-positions of the benzene ring on the S, thus resulting in low radical intensity [28].

Figure 6 presents the ESR spectrum of S radicals produced in the presence of $Al(OTf)_3$ cocatalyst. The ESR spectrum shows six lines which are due to S radicals. There is an increase in intensity of the lines which may be attributed to an increase in radical stability of the S radical. The change in intensity of spectrum and the increase in radical stability may be due to the presence of $Al(OTf)_3$ which might have caused development of more interaction of the unpaired electron with the chain proton due to increased alignment of the polymer chain, thus resulting in the formation of a more stable polymer [29].

Figure 7 shows an ESR spectrum of EA radicals produced in the absence of $Al(OTf)_3$. The lines obtained may be due to the propagating radicals –CH_2C*$(COOC_2H_5)$– or –CH_2C*$(COOC_2H_5)$–.

The spectrum for EA in Fig. 8 is a nine-line signal which may be due to effect of the growing polymer radical resulting in overlap of four and five lines due to the methylene protons having different splitting constants such that the rotation of

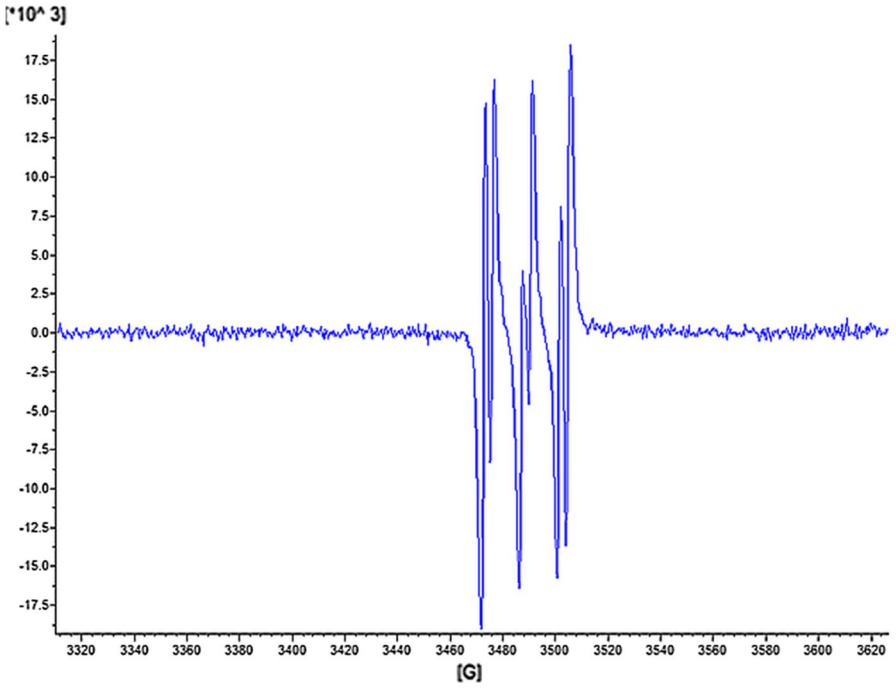

Fig. 6 ESR spectrum of S with $Al(OTf)_3$

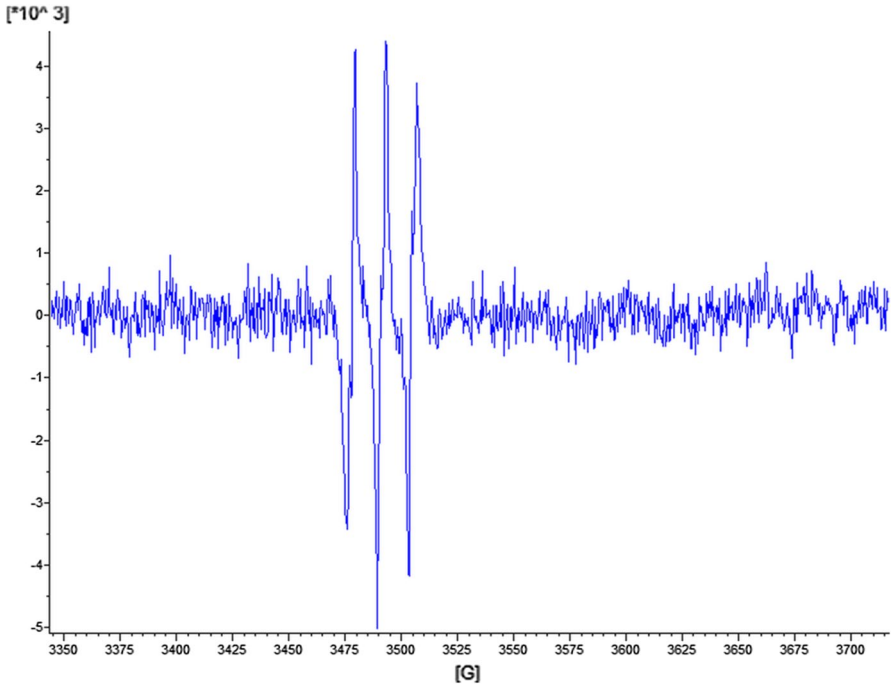

Fig. 7 ESR spectrum of EA without $Al(OTf)_3$

the end radical is not fast enough to make the methylene protons equivalent [30]. The interaction of the methylene protons with the unpaired electron is limited by rotational restrictions such that interaction can only occur on the five β protons [31]. The other line signals may have been due to the Zeeman effect and also due to the possibility of the presence of two exchangeable conformations in the polymer chain. The hindered rotation might also have been caused by increased stability of the growing polymer chain radical brought about by the presence of anionic constituents, triflate ions, resulting in increased intensity [32]. Radical migrations from propagating radicals to mid-chain radicals through a 1.5 hydrogen shift about the α carbon which might also have caused the nine-line spectrum.

Copolymers have various ends of propagating radicals due to the penultimate unit effects; thus, there is a possibility of a radical forming on the S group or the EA group [27].

The spectrum of the copolymer showed a triplet of doublets which might have been due to the hyperfine splitting interactions of the methylene radicals and methane radicals from the S radical $–CH_2CH^*Ph–$ as shown in Fig. 9. The doublet of triplets might have been due to the hyperfine splitting arising from interaction of the unpaired electron with a magnetic nucleus from neighboring atoms. There might also have been π interaction from the p orbitals of the phenyl ring of the S molecule, thus restricting rotation and stabilizing the radical [33]. Steric hindrance might also have occurred about the α and β bonds of the carbon atoms,

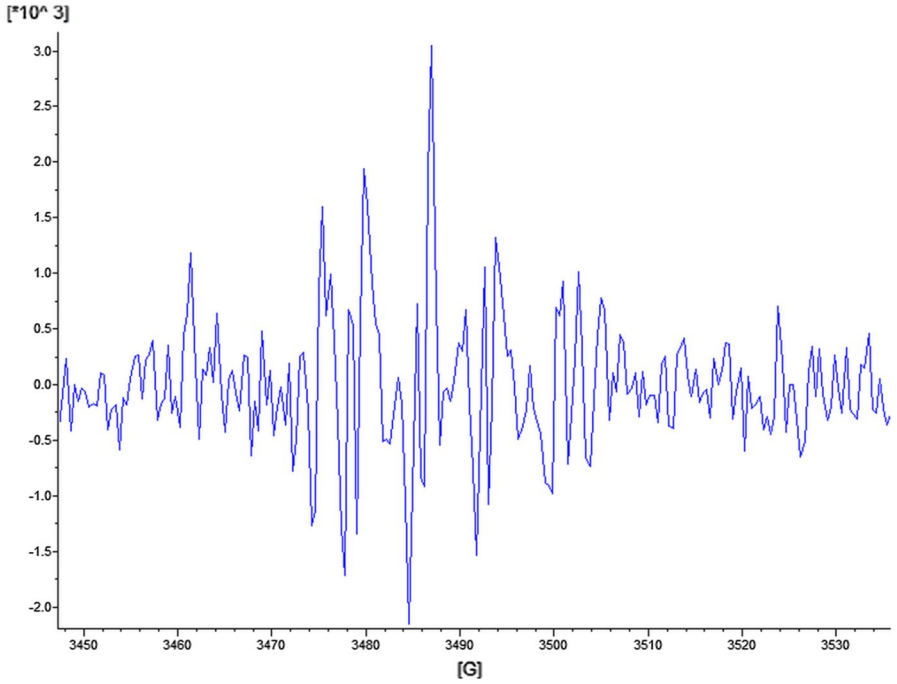

Fig. 8 ESR spectrum of EA with $Al(OTf)_3$

thus influencing radical stability with the presence of triflates being a contributing factor.

Figure 10 shows a triplet of quartets or a twelve-line spectrum which might have been caused by splitting of methylene protons of the EA radical, i.e., the rate of rotation of the end radical is equivalent due to the presence of S within the copolymer [34]. Splitting might also have occurred due to interaction between the unpaired electron of the acrylate radical and the electrons from neighboring nucleus. Polymers synthesized from ATRP contain terminal C–X bonds which can be cleaved by metallic catalysts to produce various radicals which might contributed to the increase in line signals. Most acrylate polymers undergo a hydrogen shift which is typical of a decrease in stability of the radical which can be justified by the decrease in intensity of the radicals [27, 30].

Generally, the effect of $Al(OTf)_3$ on the stability of the radical species was proven to be undeniable by the EPR studies. Although it is suggested that S polymerization is eventually promoted indirectly by the coordinated triflate–EA complex, the ESR studies showed that an S radical can also be stabilized by $Al(OTf)_3$. The longevity of S radicals is therefore also promoted by $Al(OTf)_3$. The authors could not find the literature that describes the potential direct interaction between the triflate and styryl radical. One can, however, infer that the radical must also interact with the vacant *d*-orbital of the aluminum atom.

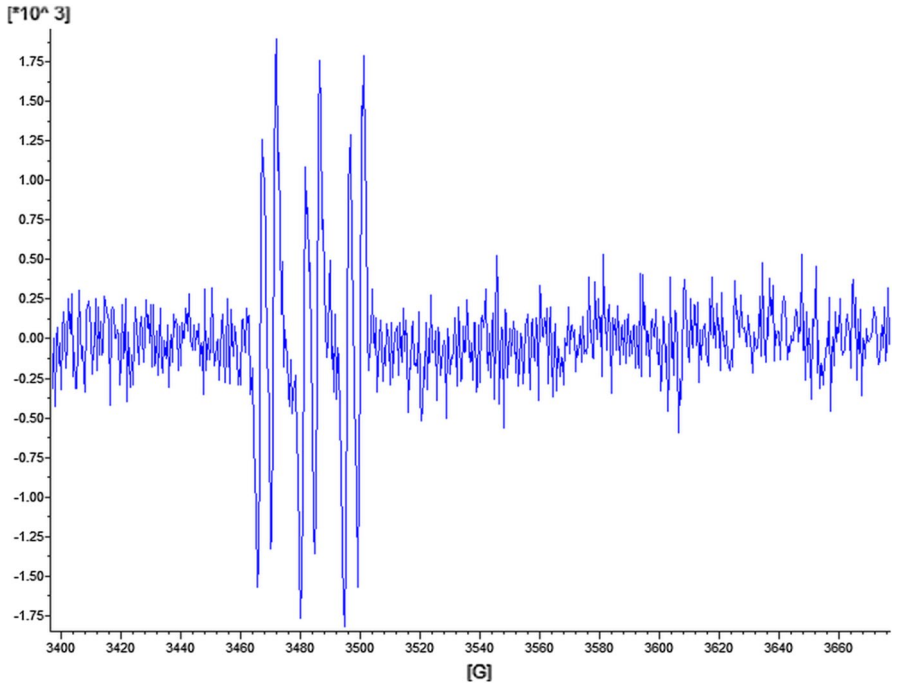

Fig. 9 ESR spectrum of the monomer mixture during a reaction in the presence of $Al(OTf)_3$

Kinetics

Both homo- and copolymerizations were performed in the presence or absence of the cocatalyst. The homopolymerization results are discussed first. Several reaction order plots were fitted, and none of these showed a significantly appropriate fit. However, they did show the effect of the triflate cocatalyst as an accelerant of conversion. Figure 11 shows the time-dependent conversion for various monomer systems.

Figure 11 indicates that the triflate only had a slight effect on the conversion rates of EA. However, S conversion showed an increase in the rate of conversion of almost three times with addition of the triflate with the 0-order rate constant increasing from 0.066%/min ($R^2 \sim 0.90$) to 0.17%/min ($R^2 \sim 0.90$). EA reacted very quickly and was therefore virtually unaffected by the triflate as far as conversion is concerned. In previous reports on copolymerization kinetics of S and EA [2], it was shown that EA reacted faster than S in bulk polymerizations. As S feed increased in these reactions, the overall polymerization rate also decreased since less S was converted.

From the results presented here, one can conclude that the same behavior is seen for S and EA homopolymerizations, concerning conversions rates, and that $Al(OTf)_3$ could have a significant effect on the conversion of S which would otherwise have a dampening effect on overall polymerization rate.

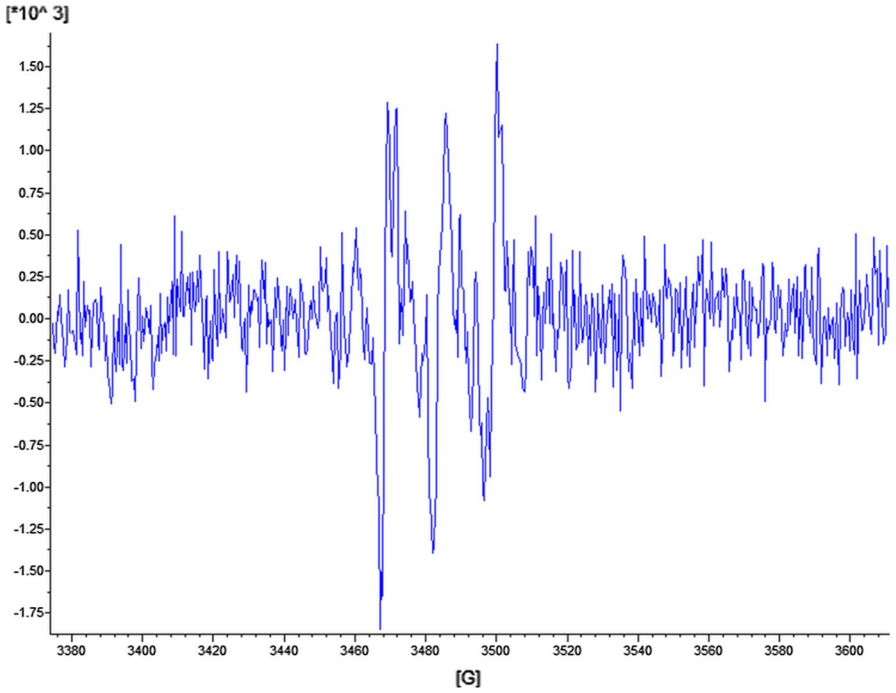

Fig. 10 ESR spectrum of the mixture of S and EA during a reaction in the absence of $Al(OTf)_3$

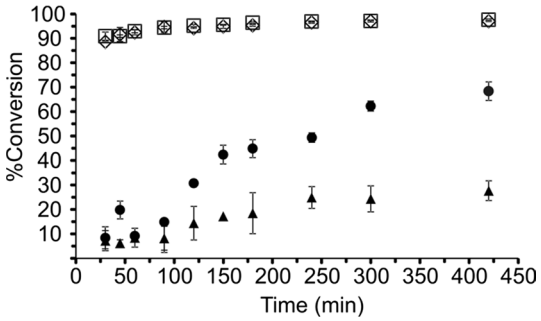

Fig. 11 Time-dependent conversion of monomers (diamond: EA, square: EA-triflate, black triangle: S and black circle: S-triflate)

It is noticed that EA conversion was again virtually unaffected by the presence of the triflate. However, the conversion of EA was significantly lower in copolymerization reactions than in the homopolymerization reactions and achieved only 53% conversion with addition of triflate as the cocatalyst. Conversely, S showed a significant sensitivity toward $Al(OTf)_3$ in the homopolymerization as observed by the marked increase in conversion which reached 85%, 20% higher than without the triflate during the same period.

In the comonomer mixture, a higher final conversion was also achieved for S compared to the homopolymerization. In the homopolymerization without triflate,

conversion reached ~ 27%, whereas it attained ~ 65% in the copolymerization reaction. With addition of $Al(OTf)_3$ to the comonomer mixture, the conversion was also ~ 17% higher than for the case of homopolymerization of S. The molecular weight is plotted as a function of conversion in Fig. 12.

Figure 12 shows that the increase in S conversion in the presence of the triflate determines the final copolymer molecular weight. If S conversion was not accelerated, the copolymer molecular weight will stabilize at ~ 40 kg/mol with an approximate 1:1 monomer conversion. It can be inferred that compositional drift will occur as soon as S is converted in the presence of $Al(OTf)_3$ due to higher S conversion and the limited effect on EA conversion.

From the discussion in Introduction, it is proposed that the coordination of the triflate with EA induces the nucleophilic attack of S which is now energetically favored compared to reactions without triflate. Subsequently, the copolymers will have a higher incorporation of S due to its higher reactivity. Reactivity ratio studies could be performed in future to confirm if cross-propagation between the monomers is improved by the triflate. Nonetheless, it would seem that the copolymer chains will exhibit a more even distribution of the comonomer due the reaction in the presence of $Al(OTf)_3$.

Molecular weight

Since the rate of conversion of S was seen to be significantly enhanced in the presence of $Al(OTf)_3$, it was investigated whether a complimentary increase in molecular weight was observed as well. Figure 13 depicts the findings for a copolymer produced from a 1:1 molar ratio of S/EA reaction feed.

On average, the triflate resulted in an approximately 50% increase in molecular weight values at corresponding time points. From the monomer conversion studies above, this could be ascribed to the increase in S conversion rate. Even though EA conversion was slower in the copolymerization reaction than in corresponding homopolymerization, the total monomer conversion was higher due to the S-triflate accelerated conversion. The increased rate of polymerization is again attributed to the increase in the reactivity of S. Therefore, the EA conversion results can be misleading in the sense that no effect could be observed from the presence of $Al(OTf)_3$.

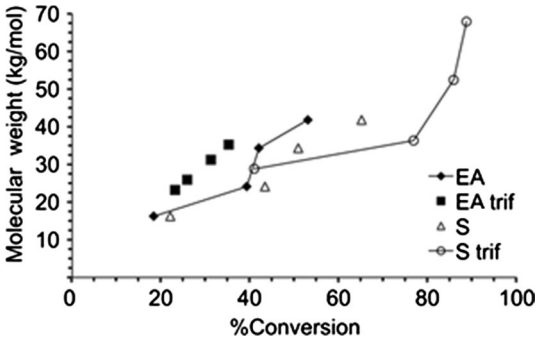

Fig. 12 $\overline{M}_n$ of the copolymers as they evolve with monomer conversion

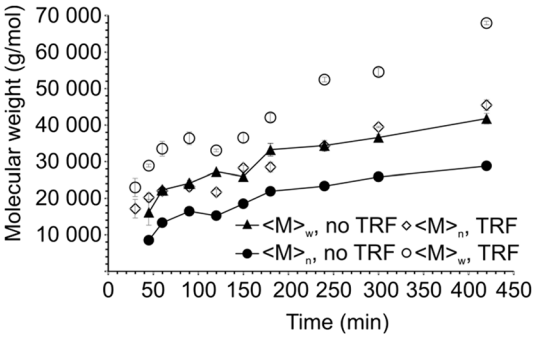

Fig. 13 $\overline{M}_n$ and $\overline{M}_w$ of the copolymers produced from the 1:1 monomer ratio reaction feed in the absence or presence of $Al(OTf)_3$

However, the effect of $Al(OTf)_3$ coordination to EA induces the nucleophilic attack of S in order to facilitate copolymerization which is now energetically more favorable than without the cocatalyst. Subsequently, a greater extent of comonomer conversion was observed which coincided with significant increases in both $\overline{M}_n$ and $\overline{M}_w$.

The fact that $\overline{M}_n$ increased points to an increase in radical lifetime in the presence of the triflate since it is an indication of the number of propagating radicals. The fact that $\overline{M}_w$ correspondingly also increased in the presence of the triflate indicated that the radical also persisted for a longer period of time to assemble more monomer units, thus increasing the length of each chain. Thus, the cocatalyst illustrated the desired increase in polymer molecular weight and higher yields of high molecular weight polymers for a given conversion. Presence of $Al(OTf)_3$ narrowed the molecular weight distributions (MWDs) of the copolymers as evidenced by the average polydispersity indices (PDIs) that range from 1.3 to 15 as compared to copolymers made in the absence of $Al(OTf)_3$ with PDIs ranging from 1.4 to 1.9 (Fig. S15). The fact that PDI remained in the range 1.3–1.5 over the 420-min reaction period indicated that the presence of triflate gave rise to copolymers with well-defined chemical composition and reproducible molecular weights.

Compositional analysis

The composition of the copolymers was established by NMR. Table 1 presents results of selected copolymers synthesized under the same reaction conditions in the absence or presence of varying amounts of the cocatalyst.

Table 1 Compositional analysis of selected copolymers synthesized with varying amounts of triflate

$f_{S,\text{ reactant}}$	$Al(OTf)_3$ amount (mol%)	F_{EA} (%)	F_S (%)
0.5	0	41.12	58.88
0.5	0.9	40.59	59.41
0.5	1.8	39.12	60.88
0.5	2.7	37.26	62.74

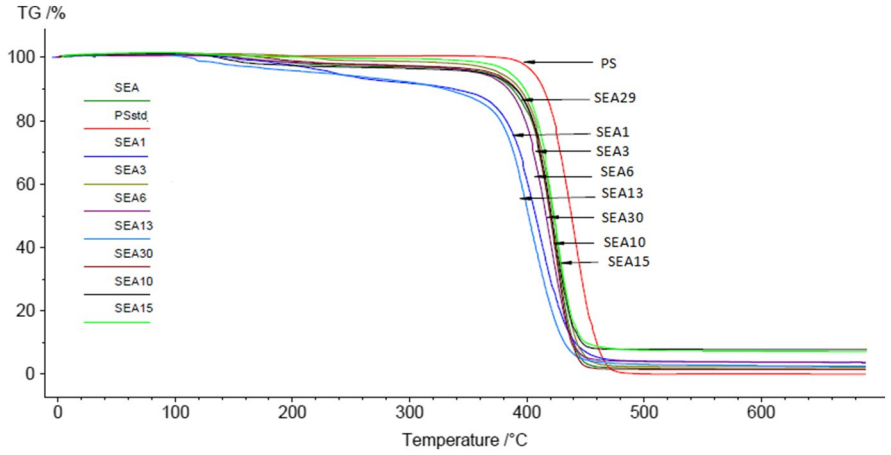

Fig. 14 Thermogravimetric traces of PS and the copolymers

Table 2 Glass transition (T_g) values for homopolymers and the copolymers

Sample	$f^{a}_{S,\ reactant}$	F^{b}_{S}	T_g (°C)
PS	–	–	100.7
SEA 15	0.8	0.838	92.5
SEA 3	0.7	0.751	81.4
SEA 10	0.7	0.748	80.6
SEA 29	0.5	0.721	76.1
SEA 6	0.4	0.647	68
SEA 1	0.5	0.608	53
SEA 13	0.4	0.541	42.7
PEA	–	–	– 23

$f^{a}_{S,\ reactant}$ is the mole fraction of styrene in feed; F^{b}_{S} is the mole fraction of styrene in copolymer

Our earlier findings on the kinetics of the cocatalyzed reactions are further supported as a compositional drift can be noticed with increase in the amount of the cocatalyst. This can be attributed to the higher S conversion and the limited effect on EA conversion in the presence of $Al(OTf)_3$.

Thermal analysis of the polymers

The thermal behavior of polystyrene (PS) and the poly(styrene-*co*-ethyl acrylate) copolymers was studied using thermogravimetry and differential scanning calorimetry analyses. Figure 14 shows the thermograms of PS and selected SEA copolymers with various S and EA compositions (Table 2). The thermograms obtained were of similar nature all having a one-step decomposition. Most of the polymeric materials were stable up to a temperature of 200 °C and started losing weight beyond this

temperature. Incorporation of EA into the polymer resulted in earlier decomposition of the copolymer as evidenced by a decrease in initial decomposition temperatures (Fig. 14). Glass transition temperatures (T_g) of the polymers were obtained following DSC analysis, and the results are presented in Table 2. Polystyrene had the highest T_g value, but as EA amounts were incrementally incorporated into the polymer, the resultant copolymer T_g values decreased approaching the homopolymer T_g value of −23 °C. These data provide further evidence of successful formation of poly(styrene-*co*-ethyl acrylate).

Conclusion

$Al(OTf)_3$ illustrated one of the first successful applications as a cocatalyst in the copolymerization of S and EA. It was established that the triflate could have numerous effects on the copolymerization.

Firstly, the coordination of $Al(OTf)_3$ to EA was observed and confirmed currently available literature reports. Although not apparent from monomer conversion studies, this EA coordination promoted S conversion by inducing a nucleophilic attack from the S monomer vinyl electrons due to the electron withdrawal from the EA vinyl group.

Secondly, ESR showed that radicals produced from either S or EA showed significant splitting patterns in the presence of a radical trap experiment. The intensity of these spectra showed that the presence of $Al(OTf)_3$ enhances the radical stability of both species and subsequently increases the longevity of both radical species.

Due to the two mechanisms mentioned here, the third important observation was made for copolymerization in the presence of $Al(OTf)_3$, namely more efficient reactions. (Co-) monomer conversion and proportional increases in molecular weights could be illustrated and confirmed one of the first successful employments of $Al(OTf)_3$ as a cocatalyst for the copolymerization of an apolar and polar vinyl monomer.

Due to the successful application of $Al(OTf)_3$ and the high abundance of aluminum in the earth crust, the authors demonstrated that a significantly more cost-effective triflate can be used as an alternative to rare earth lanthanide triflates.

References

1. Chen Y, Sen A (2009) Effect of Lewis acids on reactivity ratios for meth(acrylate)/nonpolar alkene copolymerizations. Macromolecules 42:3951–3957. https://doi.org/10.1021/ma900450p
2. McManus NT, Penlidis A (1996) A kinetic investigation of styrene/ethyl acrylate copolymerization. J Polym Sci Part A Polym Chem 34:237–248. https://doi.org/10.1002/(SICI)1099-0518(19960130)34:2<237::AID-POLA10>3.0.CO;2-R
3. Mahdi Abdollahi M, Shahram Mehdipour-Ataei S, Farshid Ziae F (2007) Using ^{1}H-NMR spectroscopy for the kinetic study of the in situ solution free-radical copolymerization of styrene and ethyl acrylate. J Appl Polym Sci 105:2588–2597. https://doi.org/10.1002/app.26290
4. Corma A, García H (2003) Lewis acids: from conventional homogeneous to green homogeneous and heterogeneous catalysis. Chem Rev 103:4307–4365. https://doi.org/10.1021/cr030680z

5. Kobayashi S, Nagayama S, Busujima TJ (1998) Lewis acid catalysts stable in water. Correlation between catalytic activity in water and hydrolysis constants and exchange rate constants for substitution of inner-sphere water ligands. Am Chem Soc 120:8287–8288. https://doi.org/10.1021/ja980715q
6. Koito Y, Nakajima K, Kobayashi H, Hasegawa R, Kitano M, Hara M (2014) Slow reactant-water exchange and high catalytic performance of water-tolerant Lewis acids. Chem Eur J 20:8068–8075. https://doi.org/10.1002/chem.201400240
7. Amer I, Young DA (2013) Chemically oxidative polymerization of aromatic diamines: the first use of aluminium-triflate as co-catalyst. Polymer 54:505–512. https://doi.org/10.1016/j.polymer.2012.11.078
8. Amer I, Young DA, Vosloo HCM (2013) Chemical oxidative polymerization of *m*-phenylenediamine and its derivatives using aluminium triflate as co-catalyst. Eur Polym J 49:3251–3260. https://doi.org/10.1016/j.eurpolymj.2013.06.031
9. Isobe Y, Fujioka D, Habaue S, Okamoto YJ (2001) Efficient Lewis acid-catalyzed stereocontrolled radical polymerization of acrylamide. Am Chem Soc 123:7180–7181. https://doi.org/10.1021/ja0158881
10. Nagel M, Poli D, Sen A (2005) Lewis acid-mediated copolymerization of methyl acrylate and methyl methacrylate with 1-alkenes. Macromolecules 38:7262–7265. https://doi.org/10.1021/ma050705r
11. Luo R, Sen A (2007) Rate enhancement in controlled radical polymerization of acrylates using recyclable heterogeneous Lewis acid. Macromolecules 40:154–156. https://doi.org/10.1021/ma062341o
12. Isobe Y, Nakano T, Okamoto YJ (2001) Stereocontrol during the free-radical polymerization of methacrylates with Lewis acids. Polym Sci A Polym Chem 39:1463–1471. https://doi.org/10.1002/pola.1123
13. Amer I, Young DA, Vosloo HCM (2014) Using aluminium triflate as co-catalyst for the polymerization of *o*-phenylenediamine and its derivatives. Polym Int 63:1229–1237. https://doi.org/10.1002/pi.4628
14. Lutz JF, Jakubowski W, Matyjaszewski K (2004) Controlled/living radical polymerization of methacrylic monomers in the presence of Lewis acids: influence on tacticity. Macromol Rapid Commun 25:486–492. https://doi.org/10.1002/marc.200300165
15. Luo R, Chen Y, Sen AJ (2008) Effects of Lewis and Brønsted acids on the homopolymerization of acrylates and their copolymerization with 1-alkenes. Polym Sci A Polym Chem 46:5499–5505. https://doi.org/10.1002/pola.22870
16. Hadjikyriacou S, Acar M, Faust R (2004) Living and controlled polymerization with alkylaluminum halides as coinitiators. Macromolecules 37:7543–7547. https://doi.org/10.1021/ma049082s
17. Belleli PG, Ferreira ML, Damiani DE (2000) Addition of Lewis bases and acids. Effects on α-olefins polymerization with soluble metallocenes, 2 propylene. Macromol Chem Phys 201:1466–1475. https://doi.org/10.1002/1521-3935(20000801)201:13<1466::AID-MACP1466>3.0.CO;2-B
18. Belleli PG, Ferreira ML, Damiani DE (2000) Addition of Lewis bases and acids. Effects on α-olefins polymerization with soluble metallocenes, 1 ethylene. Macromol Chem Phys 201:1458–1465. https://doi.org/10.1002/1521-3935(20000801)201:13<1458::AID-MACP1458>3.0.CO;2-1
19. Carlson RK, Lee RA, Assam JH, King RA, Nagel ML (2015) Free-radical copolymerisation of acrylamides, acrylates, and α-olefins. Mol Phys 113:1809–1822. https://doi.org/10.1080/00268976.2015.1015641
20. Román-Leshkov Y, Davis ME (2011) Activation of carbonyl-containing molecules with solid Lewis acids in aqueous media. ACS Catal 1:1566–1580. https://doi.org/10.1021/cs200411d
21. Fringuelli F, Pizzo F, Vaccaro L (2001) Lewis-acid catalyzed organic reactions in water. The case of $AlCl_3$, $TiCl_4$, and $SnCl_4$ believed to be unusable in aqueous medium. J Org Chem 66:4719–4722. https://doi.org/10.1021/jo010373y
22. Okuhara T (2002) Water-tolerant solid acid catalysts. Chem Rev 102:3641–3666. https://doi.org/10.1021/cr0103569
23. Wyatt PJ (1993) Light scattering and the absolute characterization of macromolecules. Anal Chim Acta 272:1–40. https://doi.org/10.1016/0003-2670(93)80373-S
24. Lee HC, Chang T (1995) On-line determination of dn/dc for size exclusion chromatography coupled with a light scattering detector. Bull Korean Chem Soc 16:640–643
25. Sage V, Clark JH, Mcquarrie DJ (2004) Supported copper triflate as catalyst for the cationic polymerization of styrene. J Catal 227:502–511. https://doi.org/10.1016/j.jcat.2004.08.013

26. Yamada B, Kageoka M, Otsu T (1992) ESR study of the radical polymerization of styrene. Macromolecules 25:4828–4831. https://doi.org/10.1007/BF00944835
27. Kajiwara A (2008) ESR study of the fundamentals of radical. JEOL News 43:39–49
28. Odian G (2004) Principles of polymerization, 4th edn. Wiley, Hoboken
29. Tsarevsky NV, Matyjaszewski K (2007) Green atom transfer radical polymerization: from process design to preparation of well-defined environmentally friendly polymeric materials. Chem Rev 107:2270–2299. https://doi.org/10.1021/cr050947p
30. Fillipov A, Chernikova E, Golubev V, Gryn'ova G, Lin C, Coote ML (2012) Use of spin trap technique for kinetic investigation if elementary steps of RAFT polymerization. In: Kokorin AI (ed) Nitroxides: theory, experiment and applications. Rijeka, Croatia, pp 407–436
31. Lund A, Danilczuk M (2012) Monomer and polymer radicals of vinyl compounds: EPR and DFT studies of geometric and electronic structures in the adsorbed state. Spectrochim Acta Part A Mol Biomol Spectrosc 98:367–377. https://doi.org/10.1016/j.saa.2012.08.054
32. Drockenmuller E, Lamps J, Catala J (2004) Living/controlled radical polymerization of ethyl and *n*-butyl acrylates at 90 °C mediated by sulfinyl nitroxides: influence of the persistent radical stereochemistry. Macromolecules 37:2076–2083. https://doi.org/10.1021/ma0351221
33. Anseth KS, Anderson KJ, Bowman CN (1996) Radical concentrations, environments, and reactivities during crosslinking polymerizations Macromol. Chem Phys 197:833–848. https://doi.org/10.1002/macp.1996.021970306
34. Tao Y, He J, Wang Z, Pan J, Jiang H, Chen S, Yang Y (2001) Synthesis of branched polystyrene and poly(styrene-*b*-4-methoxystyrene) by nitroxyl stable radical controlled polymerization. Macromolecules 34:4742–4748. https://doi.org/10.1002/macp.1996.021970306